Excitation of Several Important Metastable States of N_2 by Electron Impact

Walter L. Borst

Department of Physics, Southern Illinois University, Carbondale, Illinois 62901[*]

and Department of Physics, University of Pittsburgh, Pittsburgh, Pennsylvania 15213

Absolute cross sections for excitation of the $A\,{}^3\Sigma_u^+$, $a\,{}^1\Pi_g$, and $E\,{}^3\Sigma_g^+$ metastable states of N_2 were deduced from previous time-of-flight studies of metastable nitrogen molecules. The cross section for *direct* excitation of the $A\,{}^3\Sigma_u^+$ state was determined from threshold to 40 eV and was found to have a peak value of $(5.3^{+4.0}_{-3.0}) \times 10^{-17}$ cm^2 near 11 eV. The *total* apparent cross section of the $A\,{}^3\Sigma_u^+$ state was obtained by adding cascade contributions from the $B\,{}^3\Pi_g$ and $C\,{}^3\Pi_u$ states and was found to have a value of about 1.2×10^{-16} cm^2 at the two peaks near 11.0 and 14.5 eV. The $E\,{}^3\Sigma_g^+$ state was efficiently excited near threshold and exhibited a resonancelike excitation function with a half-width (full width of half-maximum) at about 0.4 eV and a peak cross section of $(7.0 \pm 4.0) \times 10^{-18}$ cm^2 at 12.2 eV. The excitation function for the $a\,{}^1\Pi_g$ state was obtained from threshold to about 40 eV and was found to differ markedly from two other measurements. Using the present results, a sample vibrational distribution for non-interacting molecules in the $A\,{}^3\Sigma_u^+$ state was calculated at selected electron energies near threshold. For most energies, the lowest vibrational levels are most strongly populated in qualitative agreement with atmospheric observations.

I. INTRODUCTION

Several metastable states of N_2 are excited efficiently by electron impact at low energies. Because of their large cross sections, the most important metastable states of N_2 are $A\,{}^3\Sigma_u^+$, $a\,{}^1\Pi_g$, and $E\,{}^3\Sigma_g^+$. These states are readily excited by the large nonthermal electron fluxes encountered in the earth's upper atmosphere under auroral conditions. In particular, emissions[1] from the $A\,{}^3\Sigma_u^+$ (Vegard-Kaplan system)[2,3] and $a\,{}^1\Pi_g$ states (Lyman-Birge-Hopfield system)[4] have been observed in auroras. The interpretation of rocket and ground-based observations was often rendered uncertain because of the lack of absolute excitation cross sections for these states. For instance, the vibrational distribution in the $A\,{}^3\Sigma_u^+$ state depends critically on the relative contributions from direct and cascade processes populating the vibrational levels. Although the cascade contributions can now be fairly well assessed with the aid of known excitation cross sections and transition probabilities for the $B\,{}^3\Pi_g$ and $C\,{}^3\Pi_u$ states,[5-7] as well as for other states such as the $W\,{}^3\Delta_u$ state,[8-10] there exists no measurement for the absolute cross section for direct excitation of the $A\,{}^3\Sigma_u^+$ state. It was attempted in the present study to obtain this cross section and thus be able to assess the contribution of direct excitation of the $A\,{}^3\Sigma_u^+$ state. In the course of this work it was also possible to obtain cross sections for excitation of the $a\,{}^1\Pi_g$ and $E\,{}^3\Sigma_g^+$ metastable states. As a result there appears to be some disagreement in the shape of the excitation function for the $a\,{}^1\Pi_g$ state if the present results are compared with two other existing measurements.[11,12] The absolute cross section for excitation of the $E\,{}^3\Sigma_g^+$ has been reported recently[13] and is included in the present summary. Because of the smaller cross section and the narrowness of the excitation function, this state appears to be less important in atmospheric processes. However, it remains to be seen whether or not the high excitation energy of this state affects the chemistry of the atmosphere under auroral conditions.

In the following the methods employed in arriving at absolute metastable excitation cross sections are outlined. This is followed by a summary of experimental results. The results and their applications are then discussed and a sample vibrational distribution in the $A\,{}^3\Sigma_u^+$ state for excitation by monoenergetic electrons is presented.

II. METHOD AND RESULTS

A. Decomposition of Total Metastable Excitation Function

The results presented below were extracted from the total metastable excitation function of N_2 (Fig. 1) using measured lifetimes for the $a\,{}^1\Pi_g$ and $E\,{}^3\Sigma_g^+$ states,[14] time-of-flight measurements of the relative contributions from the $A\,{}^3\Sigma_u^+$ and $a\,{}^1\Pi_g$ states, and the known response of the metastable detector to the various metastables in question.[15] In the case of the $A\,{}^3\Sigma_u^+$ state a detailed analysis of cascade contributions had to be made. The experimental technique and results such as in Fig. 1 have been reported previously.[14,16] Therefore, only an outline of the computational methods used in obtaining the present results is given in the following.

The total metastable excitation function in Fig. 1 is mainly composed of contributions from the $A\,{}^3\Sigma_u^+$, $a\,{}^1\Pi_g$, and $E\,{}^3\Sigma_g^+$ states. These contributions could be separated because of the different lifetimes
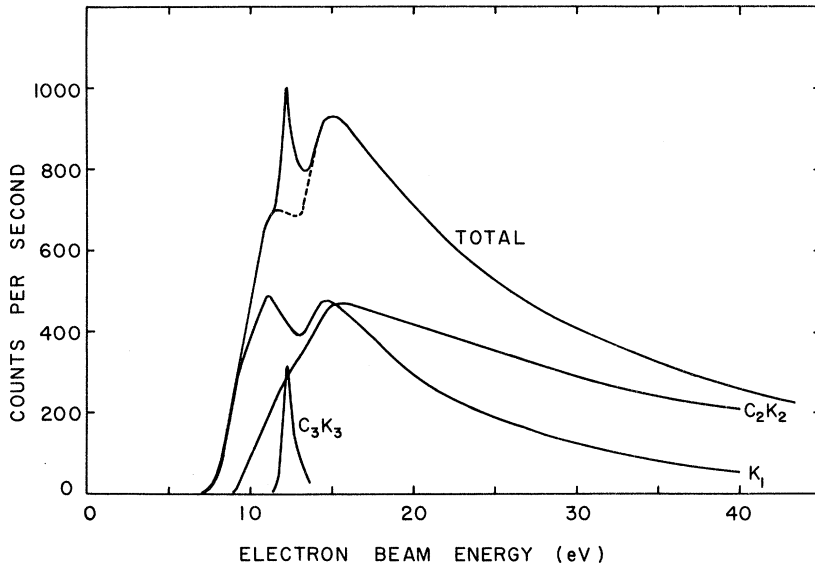
FIG. 1. Decomposition of the total metastable excitation function of N_2. The curves marked K_1, C_2K_2, and C_3K_3 represent the contributions from the $A\,^3\Sigma_u^+$, $a\,^1\Pi_g$, and $E\,^3\Sigma_g^+$ metastable states, respectively. (See text for details concerning corrections, in particular for curve K_1.) The metastable detector was located a distance 6.5 cm from the source region and consisted of a Cu–Be–O surface.

of these states.[14] The total signal count rate at the metastable detector integrating over all metastable transit times was given by

$$S(E) = K_1(E) + C_2 K_2(E) + C_3 K_3(E) ,\qquad (1)$$

where the functions $K_1(E)$, $C_2 K_2(E)$, and $C_3 K_3(E)$ are the signal count rates as a function of electron beam energy E due to the $A\,^3\Sigma_u^+$, $a\,^1\Pi_g$, and $E\,^3\Sigma_g^+$ states, respectively. The constants C_2 and C_3 represent the fractions of metastables in the $a\,^1\Pi_g$ and $E\,^3\Sigma_g^+$ states, respectively, that are able to reach the detector and thus account for in-flight metastable decay due to finite lifetime. The quantities $K_1(E)$, $K_2(E)$, and $K_3(E)$ are the signal count rates that would be measured for infinite metastable lifetimes. The lifetime for the $A\,^3\Sigma_u^+$ state $(\tau \sim 1 \text{ sec})^{17}$ is infinite for the purposes of this experiment and therefore $C_1 = 1$. The fractions C_2 and C_3 were calculated from

$$C = \int_0^\infty \frac{1}{t^4} \exp\left(-\frac{\beta}{t^2} - \frac{t}{\tau}\right) dt \Big/ \int_0^\infty \frac{1}{t^4} \exp\left(-\frac{\beta}{t^2}\right) dt ,\qquad (2)$$

where t is the metastable transit time, β an experimentally known constant,[14] and τ the lifetime of the metastable state. For the $a\,^1\Pi_g$ state, C_2 was calculated using Eq. (2) and found to be about 0.3, assuming a lifetime[14] $\tau = 115$ μsec and a distance of 6.5 cm between detector and source.

The contribution $C_3 K_3(E)$ in Eq. (1) due to the $E\,^3\Sigma_g^+$ state could be assessed rather accurately by varying the detector distance and/or changing the detector surface. For large detector distances and appropriate detector surfaces, the contribution from the $E\,^3\Sigma_g^+$ state was negligible and as a result the dashed part in the total metastable excitation func-

tion in Fig. 1 was obtained. The details entering in the determination of the dashed part in Fig. 1 and the excitation function of the $E\,^3\Sigma_g^+$ state are beyond the scope of this paper and will be reported separately.[13] After subtracting the E-state contribution $C_3 K_3(E)$, Eq. (1) reduces to a signal count rate

$$S'(E) = K_1(E) + C_2 K_2(E) .\qquad (3)$$

In Eq. (3) the quantities S' and C_2 are known. The ratio

$$R(E) = K_2(E)/K_1(E)\qquad (4)$$

was obtained as a function of energy in a previously reported time-of-flight measurement.[14] Combining Eqs. (3) and (4) yields the excitation functions

$$K_1(E) = S'(E)/[1 + C_2 R(E)]\qquad (5)$$

and

$$K_2(E) = S'(E) R(E)/[1 + C_2 R(E)]\qquad (6)$$

for the $A\,^3\Sigma_u^+$ and $a\,^1\Pi_g$ states (see Fig. 1). The absolute excitation cross section $\sigma_2(E)$ for the $a\,^1\Pi_g$ state is related to the function $K_2(E)$ by

$$K_2(E) = (I_b/e)\,nl\,(\Omega/4\pi)\,[\gamma_{v'}]_q \sigma_2(E) ,\qquad (7)$$

where I_b is the electron beam current averaged over the period of the beam pulse, e is the electronic charge, n the density of N_2 in the gas source,[14] l the effective scattering length of the collision chamber, Ω the solid angle subtended by the metastable detector at the center of the collision chamber, $[\gamma_{v'}]_q$ the "Franck-Condon weighted" secondary electron yield, and $\sigma_2(E)$ the excitation cross section at an electron energy E. The "Franck-Condon weighted" yield was calculated from the expres-
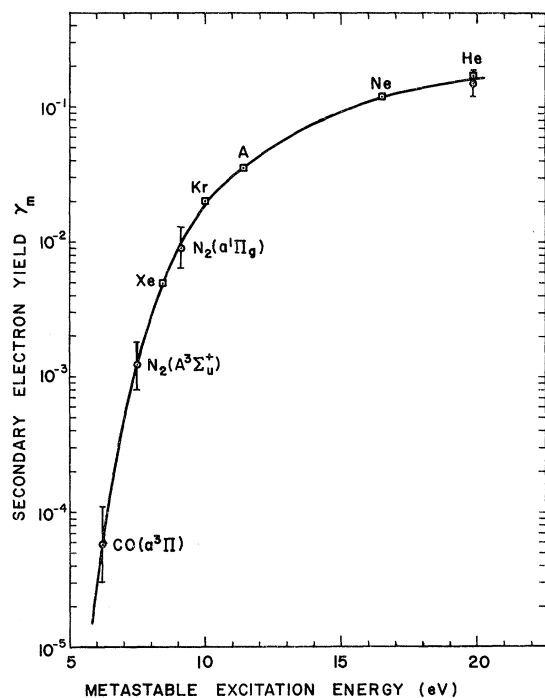
FIG. 2. Secondary electron yields for Auger ejection
of electrons from a Cu-Be-O surface by thermal metastables.
For the molecular states listed the excitation energy was
somewhat arbitrarily chosen as the energy of the vibra-
tional level v' with the largest Franck-Condon factor for
the transition from the N_2 ($^1\Sigma_g^+$, $v'' = 0$) ground state (see
Ref. 15).

sion[15]

$$[\gamma_{v'}]_q = \sum_{v'} q_{v',0}\gamma_{v'} \,, \tag{8}$$

where $q_{v',0}$ is the Franck-Condon factor for the
transition $\chi^1\Sigma_g^+(v'' = 0) \rightarrow a^1\Pi_g(v')$ from the N_2 ground
state and $\gamma_{v'}$ is the secondary electron yield for the
v'th vibrational level of the $a^1\Pi_g$ state. Only direct
excitation of the $a^1\Pi_g$ state was taken into account in
Eq. (8). It appears that cascade effects are small
in this case. [11]

B. Secondary Electron Yields

It can be seen from Eq. (7) that, in order to de-
termine the excitation cross section, the secondary
electron yield has to be known and vice versa. Sec-
ondary electron yields for various metastables are
shown in Fig. 2. The details entering in the con-
struction of the yield curve in this figure have been
discussed elsewhere. [15] It is noted that the mea-
sured yields from the Cu-Be-O surface plotted as
a function of metastable excitation energy follow a
single smooth curve. This surprising fact implies
that to a good degree of approximation the yield is
determined by the metastable excitation energy
alone independently of the gas species. In the case

of $N_2(a^1\Pi_g)$ metastables, the yield was obtained from
Eq. (7) by using Ajello's value of 3.85×10^{-17} cm^2
for the maximum cross section at 15.5 eV. [11] Hence
the present cross section for the $a^1\Pi_g$ state is nor-
malized in magnitude to this value. Very good
agreement was found to exist in the position of the
peak in the cross section at 15.5 eV, although the
shape of the present excitation function for the $a^1\Pi_g$
state differs significantly from that reported by
Ajello.

The study of $N_2(a^1\Pi_g)$, $CO(a^3\Pi)$, and other meta-
stables served to establish the consistency in the
yield curve (Fig. 2). After finding further agree-
ment between the present and optical methods used
in determining absolute excitation cross sections, [18]
it was decided that the yield for the $N_2(A^3\Sigma_u^+)$ state
can be interpolated in Fig. 2. The yield plotted for
this state in Fig. 2 corresponds to the maximum
Franck-Condon factor ($v' = 8$, $E = 7.50$ eV). The
"Franck-Condon weighted" yields for the individual
vibrational levels of the $A^3\Sigma_u^+$ state are shown in
Fig. 3. It is seen that the original Franck-Condon
curve $q_{v',0}$ is drastically altered by the strong de-
pendence of the yield on metastable excitation en-
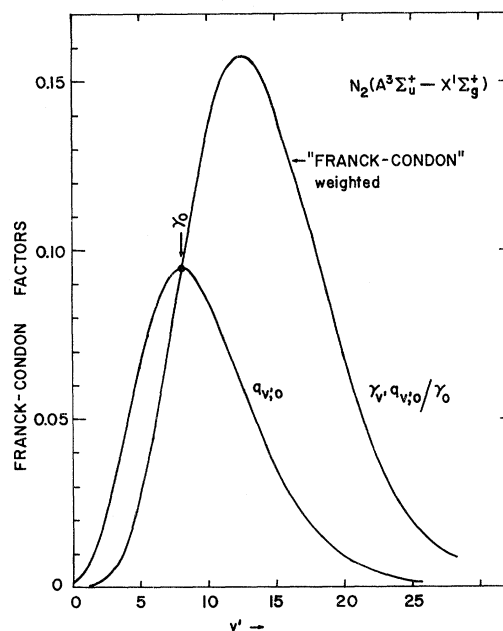ergy. The maximum in the curve $q_{v',0}$ at $v' = 8$ is

FIG. 3. Example of "Franck-Condon weighting" of
secondary electron yields. The particular case chosen
corresponds to the transition $A^3\Sigma_u^+(v') \rightarrow X^1\Sigma_g^+(v'' = 0)$ in
N_2. Franck-Condon factors for this transition are desig-
nated $q_{v',0}$. The area under the curve $q_{v',0}$ is unity. The
"Franck-Condon weighted" curve $\gamma_{v'}\cdot q_{v',0}/\gamma_0$ was normalized
to coincide with the maximum in the curve $q_{v',0}$. The experi-
mental yield $[\gamma_{v'}]_q$ is obtained by multiplying the area under
the Franck-Condon weighted curve by γ_0, where γ_0 is the
yield for $N_2(A^3\Sigma_u^+)$ plotted in Fig. 2.

shifted to $v' \simeq 12$ in the Franck-Condon weighted curve. With the normalization chosen in Fig. 3, the areas under the two curves differ by a factor of 2. This implies that the effective yield for direct excitation of the $A\,^3\Sigma_u^+$ state is twice as large as the yield γ_0 corresponding to the maximum in the Franck-Condon distribution $q_{v',0}$. Whereas the case of atomic metastables is straightforward, it is obvious that care has to be exercised in determining the effective yield for molecular states.

C. $A\,^3\Sigma_u^+$ State

The component $K_1(E)$ (Fig. 1) in the total metastable excitation function of N_2 was mainly caused by metastables in the $A\,^3\Sigma_u^+$ state. If only direct excitation contributed to the signal $K_1(E)$, the excitation cross section for this state could be obtained by substituting the effective yield $[\gamma_{v'}]_q$ for the $A\,^3\Sigma_u^+$ state from Fig. 3 into an expression exactly analogous to Eq. (7). However the curve $K_1(E)$ has two peaks indicating the presence of cascading effects and/or several very long-lived metastable states. Clearly, the $A\,^3\Sigma_u^+$ state is populated in part by cascade from the $B\,^3\Pi_g$ and $C\,^3\Pi_u$ states (first and second positive bands). Cascade from these states populates only the lowest vibrational levels of the $A\,^3\Sigma_u^+$ state to a significant degree, whereas direct excitation of the $A\,^3\Sigma_u^+$ state preferentially populates the higher level of this state, as can be seen in Fig. 3. Fortunately the present technique discriminates strongly against the lower vibrational levels of the A state by applying much larger weights $\gamma_{v'}$ on the higher vibrational levels, as is evident from the strong dependence of the yield $\gamma_{v'}$ on the excitation energy (Fig. 2). It was thus found by computation (see below) that cascade from the B and C states amounts to a contribution to the excitation function $K_1(E)$ of less than 20%. This made it possible to extract the direct excitation cross section for the $A\,^3\Sigma_u^+$ state from the function $K_1(E)$.

If cascading from the B and C states is taken into account, Eq. (7) has to be modified for the $A\,^3\Sigma_u^+$ state resulting in an *approximate* relationship of the form

$$K_1(E) = (I_b/e)\, nl\,(\Omega/4\pi)$$

$$\times \{\sigma_A(E)\,[\gamma_{v'}]_q + \sigma_B(E)\,\gamma_B(A) + \sigma_C(E)\,\gamma_C(A)\}\,, \quad (9)$$

where σ_A, σ_B, and σ_C are the direct excitation cross sections for the A, B, and C states, respectively, $[\gamma_{v'}]_q$ is the Franck-Condon weighted yield for direct excitation of the A state defined in analogy to Eq. (8), and $\gamma_B(A)$ and $\gamma_C(A)$ are the effective yields for the vibrational levels of the A state populated by cascade from the B and C states. Equation (9) is an approximation because only directly excited levels of the B and C states were assumed

to populate the A state. However this approximation is rather good because of the smallness of cross sections of other states which eventually cascade to the A state, again populating only the lower levels of this state. Since the last two terms in brackets in Eq. (9) amount to a total of less than 20% as compared to the first term, cascading from states other than the B and C states must be rather negligible under the present conditions. Another approximation contained in Eq. (9) is based on the fact that the Franck-Condon principle was assumed to hold near the thresholds of excitation. Again this is a sufficiently good approximation as far as cascading is concerned if one recalls the smallness of the last two terms in Eq. (9).

The effective secondary electron yields $\gamma_B(A)$ and $\gamma_C(A)$ appropriate for cascading from the $B\,^3\Pi_g$ and $C\,^3\Pi_u$ states were calculated from the expressions

$$\gamma_B(A) = \sum_{v''}\left(\sum_{v',0} A_{v',v''}\,\tau_{v'}\right)\gamma_{v''} \quad (10)$$

and

$$\gamma_C(A) = \sum_{v''}\left[\sum_{v'}\left(\sum_v q_{v,0} A_{v,v'}\,\tau_v\right) A_{v',v''}\,\tau_{v'}\right]\gamma_{v''}\,, \quad (11)$$

where the indices v, v', and v'' refer to the vibrational levels of the C, B, and A states, respectively, and the quantities q, A, and τ are Franck-Condon factors, transition probabilities, and lifetimes, respectively. Using values for the latter three quantities[7] and for the yields $\gamma_{v''}$ for the vibrational levels of the $A\,^3\Sigma_u^+$ state (Fig. 2), it was calculated that $\gamma_B(A) = 2.7 \times 10^{-4}$ and $\gamma_C(A) = 1.3 \times 10^{-4}$. These values are to be compared with the much larger Franck-Condon weighted yield $[\gamma_{v'}]_q = 2.5 \times 10^{-3}$ calculated with the aid of the yields in Figs. 2 and 3. This clearly shows that direct excitation of the $A\,^3\Sigma_u^+$ state is most effective in the present case and that cascading contributions are only of the order of 10% if one assumes equal values for σ_A, σ_B, and σ_C in Eq. (9).

All quantities in Eq. (9) except $\sigma_A(E)$ were known.[14] Solving Eq. (9) for the direct excitation cross section $\sigma_A(E)$ of the $A\,^3\Sigma_u^+$ state, it was found that the peak cross section occurred near 11 eV and had a value of

$$\sigma_A(11.0\text{ eV}) = (5.3\,{}^{+4.0}_{-3.0}) \times 10^{-17}\text{ cm}^2\,, \quad (12)$$

where the errors indicated are the most probable errors. The excitation function $\sigma_A(E)$ is shown in Fig. 4. It was obtained by subtracting the cascade contributions in Eq. (9) using the calculated values for $\gamma_B(A)$ and $\gamma_C(A)$, together with the cross sections $\sigma_B(E)$ and $\sigma_C(E)$ from Stanton and St. John's work.[5] It was surprising to find that after subtraction of the cascade contribution, a substantial portion of the secondary peak in the excitation function $K_1(E)$ in Fig. 1 near 15 eV remained. It appears
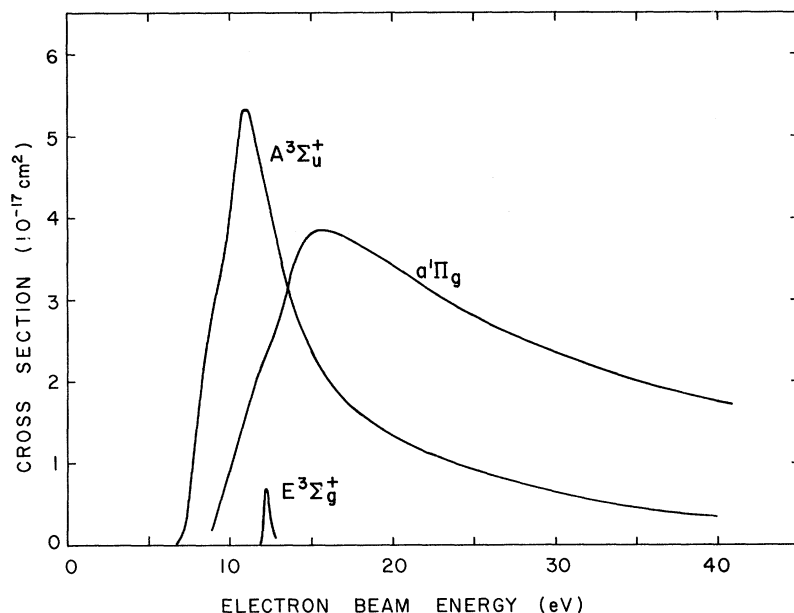
FIG. 4. Cross sections for electron-impact excitation of important metastable states of N_2. The curve for the $A\,^3\Sigma_u^+$ state is the cross section for direct excitation (see also Fig. 5). The cross section for the $E\,^3\Sigma_g^+$ state was obtained from curve C_3K_3 in Fig. 1 after correcting for the energy spread in the electron beam (Ref. 13). The cross section for the $a\,^1\Pi_g$ state was obtained from curve C_2K_2 in Fig. 1.

that this secondary peak was partly due to high-lying metastable states with thresholds near 12 eV and long lifetimes ($\tau > 0.1$ msec). Assuming a threshold of 12 eV, the cross section of the un-identified states would have to be of the order of 2×10^{-18} cm^2 in order to account for the magnitude of the secondary peak. It is possible that the non-resonant part of the excitation function of the $E\,^3\Sigma_g$ state is in part responsible for the secondary peak, since it has a threshold near 12 eV and a peak near 15 eV.[9] The resonant part of the excitation function[13] in Fig. 4 has a peak cross section of 7×10^{-18} cm^2 which according to the present measurements has to be larger than the nonresonant part. Other meta-stable states of N_2 such as the $W\,^3\Delta_u$ and $w\,^1\Delta_u$ states are believed to be of minor importance in the present case because of low excitation energies and hence low secondary electron yields. In the case of the $W\,^3\Delta_u$ state only the lowest vibrational level is sufficiently metastable to be de-tectable, but the excitation cross section for this level appears to be too small ($\sim 10^{-19}$ cm^2) to be of concern.[10] For the higher levels of the $W\,^3\Delta_u$ state, transitions to the $B\,^3\Pi_g$ state contribute via cascade to the excitation of the lower levels of the $A\,^3\Sigma_u^+$ state. But it has been shown above that this type of cascade results only in small corrections to the cross section $\sigma_A(E)$. This is particularly true for the $W\,^3\Delta_u$ state since its peak cross section seems to be only about 5×10^{-18} cm^2.[9,10]

The $a''\,^1\Sigma_g^+$ state of N_2 has the proper threshold energy of about 12.2 eV in order to contribute to the secondary peak, but it is uncertain if its lifetime is suffi-ciently long. In summary, it cannot be decided on the basis of the present measurements which par-

ticular state(s) caused the pronounced secondary peak in the function $K_1(E)$ near 15 eV. Nonetheless, this secondary structure was removed by subtrac-tion assuming a shape of the excitation function for the unidentified states similar to that for other singlet-triplet transitions in N_2. The detailed shape of the excitation function for the $A\,^3\Sigma_u^+$ state is therefore somewhat uncertain in the intermediate energy range (above 15 eV).

It is to be noted that the excitation function for the $A\,^3\Sigma_u^+$ state in Fig. 4 obtained after subtraction of the secondary peak is similar to that for the $B\,^3\Pi_g$ and $C\,^3\Pi_u$ states[5] and also to that for the $a\,^3\Pi$ state of CO,[14] as is to be expected. In particular, these excitation functions exhibit a peak about 3 eV above threshold and a half-width [full width at half-maximum (FWHM)] of about 5 eV.

D. Summary of Results

The present results of metastable excitation cross sections of N_2 are summarized in Figs. 4 and 5, and in Tables I–III. Figure 4 contains the cross sections for the three most important metastable states of N_2. The cross section for the $a\,^1\Pi_g$ state was obtained from the curve C_2K_2 in Fig. 1 and Eq. (7). It is normalized in peak value to Ajello's val-ue of 3.85×10^{-17} cm^2.[11] The resonant cross sec-tion for the $E\,^3\Sigma_g^+$ state has been reported previous-ly.[13] Figure 5 is a summary of direct and total apparent excitation cross sections for the $A\,^3\Sigma_u^+$ state. The latter cross section was obtained by adding the cascade contribution from the $B\,^3\Pi_g$ and $C\,^3\Pi_u$ states.[5] Table I lists maximum cross sec-tions and peak energies of N_2 states which were of relevance in the present work. The cross sections
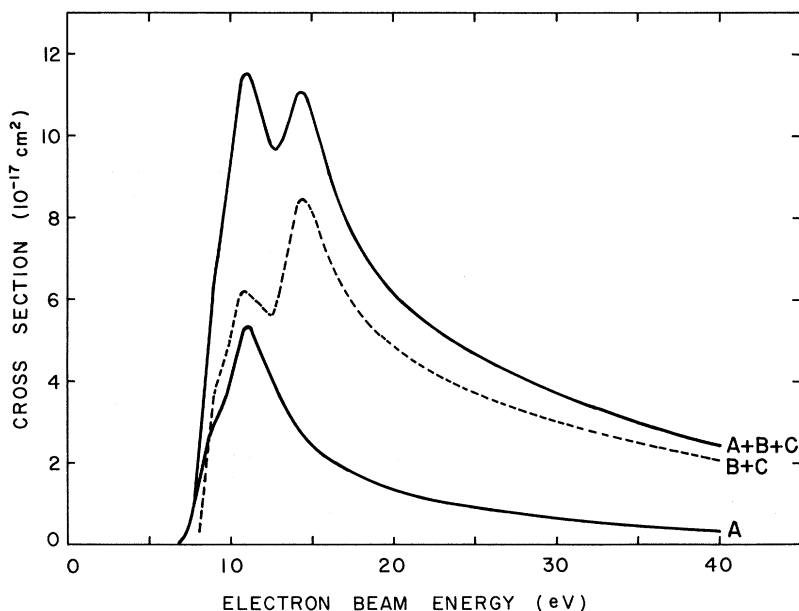
FIG. 5. Cross sections for electron-impact excitation of $N_2(A\,^3\Sigma_u^+)$. Curve A is the direct excitation cross section obtained in the present work. Curve $B+C$ is the total apparent excitation cross section for the $B\,^3\Pi_g$ state including cascading from the $C\,^3\Pi_u$ state (from Ref. 5). Curve $A+B+C$ is the sum of curves A and $B+C$ and represents the total apparent cross section for the $A\,^3\Sigma_u^+$ state including cascade from the B and C states.

for the $A\,^3\Sigma_u^+$ and $a\,^1\Pi_g$ states of N_2 obtained in the present work are tabulated in Tables II and III, re-spectively.

III. DISCUSSION

The present peak cross section of 5.3×10^{-17} cm^2 for direct excitation of the $A\,^3\Sigma_u^+$ state can be compared with an estimate of 1.8×10^{-16} cm^2 by Shemansky and Broadfoot.[7] The estimate was based on a peak cross section of 1.2×10^{-16} cm^2 for the $B\,^3\Pi_g$ state[7] and a ratio of $\sigma_A/\sigma_B = 1.5$ for the peak cross sections of the A and B states as inferred by Shemansky from electron energy-loss measurements of other investigators.[19,20] It appears, however, that a ratio of $\sigma_A/\sigma_B = 1.0$ or even smaller is equally well within the realm of accuracy of the energy-loss measurements because the estimate has to be made at nearly equal electron energies in order to circumvent problems associated with changing electron spectrometer sensitivity and this necessitates the separation of very closely spaced vibrational levels of different states. If a ratio of $\sigma_A/\sigma_B = 1.0$ is assumed together with Stanton and St. John's peak value of $\sigma_B = 6.2\times10^{-17}$ cm^2 (Table I), a value of $\sigma_A = 6.2\times10^{-17}$ cm^2 follows for the peak cross section of the $A\,^3\Sigma_u^+$ state. This agrees well with the present value. A value of $\sigma_A = 3\times10^{-17}$ cm^2 estimated by Brinkmann and Trajmar[19] is also in reasonable agreement with the present result. Theoretical calculations by Cartwright,[9] Stolarski et al.,[21] and Bauer and Bartky[22] yielded peak cross sections σ_A of about 3×10^{-16}, 4×10^{-17}, and 3×10^{-17} cm^2, respectively. Unfortunately, these values and the shapes of the theoretical excitation functions obtained in the course of these calculations are in serious disagreement and none of them resembles

the measured excitation function for the $A\,^3\Sigma_u^+$ state in Fig. 4. It is hoped that more accurate calculations are feasible in the near future. Freund's order of magnitude estimate[23] of 10^{-16} cm^2 for σ_A is certainly correct, although his assumption of constant detector sensitivity for all vibrational levels of the $A\,^3\Sigma_u^+$ state may be unrealistic as is evidenced by the present results in Figs. 2 and 3.

It was shown above that the present method emphasizes the upper vibrational levels of the $A\,^3\Sigma_u^+$ state. This may cause a slight shift in the peak of the excitation function at 11.0 eV (Fig. 4). In order to investigate this point, synthetic cross sections were constructed for individual vibrational

TABLE I. Maximum cross sections for electron-impact excitation of important molecular states of N_2.[a]

State	Comments	Cross section (10^{-17} cm^2)	Peak energy (eV)
$A\,^3\Sigma_u^+$	direct	5.3	11.0
$A\,^3\Sigma_u^+$	total	11.5	11.0
		11.0	14.5
$B\,^3\Pi_g$	total	6.2	10.8
		8.4	14.5
$C\,^3\Pi_u$	total	5.2	14.5
$a\,^1\Pi_g$	total	3.85	15.5
$E\,^3\Sigma_g^+$	resonance (mainly $v'=0$)	0.7	12.2

[a]Cross sections for the $B\,^3\Pi_g$ and $C\,^3\Pi_u$ states were taken from Stanton and St. John's work (Ref. 5). The peak cross section for the $a\,^1\Pi_g$ state is that reported by Ajello (Ref. 11).

TABLE II. Cross sections for electron-impact excitation of the $A\,^3\Sigma_u^+$ state of N_2.

Electron energy (eV)	Excitation cross section	
	Direct $(10^{-17}\,cm^2)$	Total $(10^{-17}\,cm^2)$
8	1.5	2.1
9	2.9	6.6
10	4.0	9.3
11	5.3	11.5
12	4.6	10.3
13	3.6	9.8
14	2.8	11.0
15	2.4	10.5
16	2.1	9.1
18	1.6	7.2
20	1.3	6.1
25	0.9	4.6
30	0.6	3.7
35	0.4	3.0
40	0.3	2.4

levels of the $A\,^3\Sigma_u^+$ state. It was found that a more correct position of the peak in Fig. 4 is at 10.7 eV and the peak cross section is more nearly 6×10^{-17} cm^2. The initial rise in the total metastable excitation function in Fig. 1, which was a result of direct excitation of the $A\,^3\Sigma_u^+$ state, is also shifted slightly towards higher energies. These corrections, however, were not considered further, because they were well within the limits of error of the present measurements.

Although the reverse transition $A\,^3\Sigma_u^+ \to B\,^3\Pi_g$ ("reverse first positive system"[8,24]) can redistribute the vibrational population in the $A\,^3\Sigma_u^+$ state, this was not taken into account because the upper vibrational levels of the A state have sufficiently long lifetimes[10] to be detected directly under the present conditions.

Deactivation of the $A\,^3\Sigma_u^+$ state by N_2 molecules was also found to be negligible in the pressure range of interest (10^{-4} Torr). Excited metastables thus did not interact with other molecules but were deexcited at the surface of the metastable detector or at the reaction chamber walls after a free flight of about 0.1 msec duration. Vibrational distributions in the $A\,^3\Sigma_u^+$ state in the case of noninteracting metastables were calculated using the present cross sections. The results of the calculation are shown in Fig. 6.

It is seen in Fig. 6 that the lowest vibrational levels of the $A\,^3\Sigma_u^+$ state are populated most efficiently (except for the lowest electron beam energies). This is in qualitative agreement with atmospheric observations.[2,3] Quantitative agreement between the vibrational distribution attained in the upper atmosphere during auroral conditions and the present calculations (after integrating over the

auroral electron energy spectrum) cannot be expected if deactivation effects and transitions such as the "reverse first positive system" take place. It has been reported recently by Shemansky et al.[25] that higher vibrational levels of the $A\,^3\Sigma_u^+$ state are more efficiently deactivated than the lowest ones. This would indicate that the population densities in the lower levels are further enhanced as compared to those in Fig. 6.

The excitation function of the $a\,^1\Pi_g$ state shown in Fig. 4 can be compared with measurements of Ajello[11] and Freund.[12] General agreement exists in the position of the maximum near 15.5 eV, but rather serious discrepancies prevail in the detailed shape of the excitation functions near threshold and beyond the maximum. In particular, Ajello's excitation function drops much more slowly than the present and Freund's curve shows a renewed rise beginning near 27 eV which may have been due to radiation from metastable states of N_2^+.[12]

The excitation function for the $E\,^3\Sigma_g^+$ state shown in Fig. 4 was obtained from the curve C_3K_3 in Fig. 1 using a deconvolution procedure in order to eliminate the energy spread in the electron beam.[13] The peak cross section of 7×10^{-18} cm^2 at 12.2 eV appears to be larger than anticipated.[26] There exists no other absolute measurement of this cross section. A relative measurement of the excitation function for the $E\,^3\Sigma_g^+$ state has been reported by Ehrhardt and Willmann[27] and is in good agreement with the present result. In particular, the width of the resonance was found to be about 0.4 eV (FWHM) in both cases. Complete agreement with the results of Ehrhardt and Willmann should not be expected since these authors performed an energy-loss measurement at an electron scattering angle of 20°, whereas the present measurement integrates over all scattering angles. It is interesting to note

TABLE III. Cross section for electron-impact excitation of the $a\,^1\Pi_g$ state of N_2 based on the present excitation function for this state.

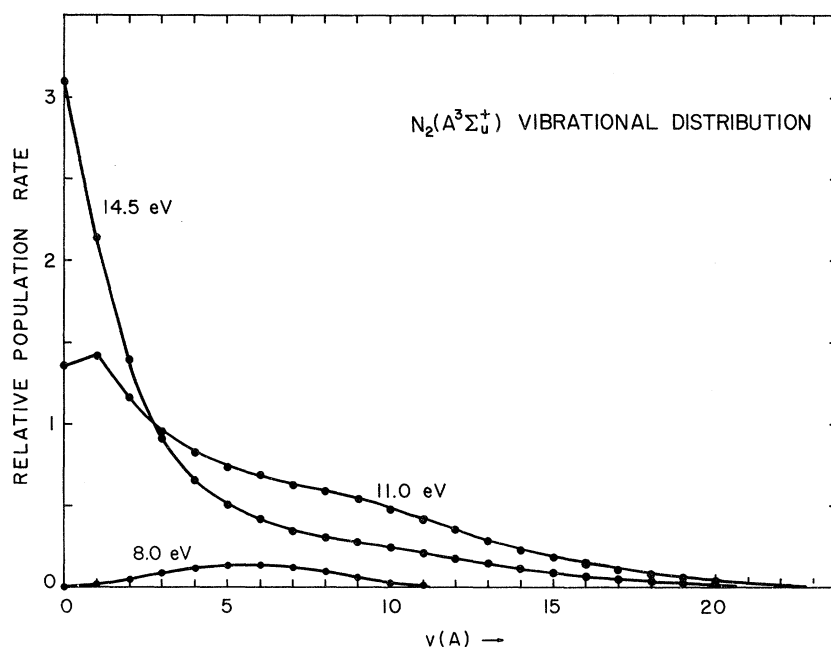| Electron energy (eV)	Cross section $(10^{-17}\,cm^2)$
9	0.15
10	0.85
12	2.2
14	3.4
16	3.85
18	3.65
20	3.4
25	2.8
30	2.35
35	2.0
40	1.75

FIG. 6. Population rates of vibrational levels of the N_2 $(A\,^3\Sigma_u^+)$ state at selected electron energies for the case of noninteracting metastables. The normalization of the curves is such that the ordinate values give the cross sections for the individual vibrational levels in units of 10^{-17} cm^2. The curves include only cascade effects from directly excited $B\,^3\Pi_g$ and $C\,^3\Pi_u$ states. The curves shown may not directly correspond to the equilibrium vibrational distribution encountered in auroras because collisions between molecules were neglible under the present conditions, and metastables were deexcited within 1 msec or less upon colliding with the walls of the reaction chamber.

that no direct evidence was found either from Ehrhardt and Willmann's or the present work, which would indicate the presence of the nonresonant part of the excitation function of the $E\,^3\Sigma_g^+$ state. Because of the narrow width and a smaller cross sectional value, this state appears to be less important in atmospheric processes than the $A\,^3\Sigma_u^+$ and $a\,^1\Pi_g$ states.

IV. SUMMARY AND CONCLUSIONS

On the basis of previous time-of-flight studies and metastable lifetime measurements, the total metastable excitation function of N_2 (Fig. 1) was decomposed into individual excitation functions for the $A\,^3\Sigma_u^+$, $E\,^3\Sigma_g^+$, and $a\,^1\Pi_g$ metastable states. Absolute excitation cross sections for these states (Figs. 4 and 5, Tables I–III) were obtained using the known sensitivity of the metastable detector (Fig. 2). The cross section for direct excitation of the $A\,^3\Sigma_u^+$ state obtained in this work appears to be the first measurement of this kind. Previous estimates of this cross section based on theoretical as well as experimental information cover a wide range of values from 0.3 to 3×10^{-16} cm^2. The present peak value of 5.3×10^{-17} cm^2 lies near the lower end of this range. Experimental evidence seems to indicate that unidentified metastable states of N_2 with thresholds near 12 eV and long lifetimes (> 0.1 msec) contributed to the second peak in the

total metastable excitation function near 15 eV (Fig. 1). Using the present cross section for direct excitation of the $A\,^3\Sigma_u^+$ state together with excitation cross sections for the $B\,^3\Pi_g$ and $C\,^3\Pi_u$ states, the total apparent cross section of the $A\,^3\Sigma_u^+$ state was obtained and found to be about 1.2×10^{-16} cm^2 at the two peaks at 11 and 14.5 eV. Vibrational distributions in the $A\,^3\Sigma_u^+$ state were calculated for selected electron beam energies near excitation threshold and showed the interplay between direct and cascade excitation of the $A\,^3\Sigma_u^+$ state. Generally, the lowest levels of the $A\,^3\Sigma_u^+$ states are most strongly populated in agreement with atmospheric observations. It is hoped that the present work is of use in atmospheric model making and in laboratory studies involving the excitation of N_2 molecules.

---

*Present address.

[1]For a review of atmospheric emissions see, for example, *Atmospheric Emissions*, edited by B. M. McCormac and A. Ohmholt (Van Nostrand and Reinhold, Princeton,

N. J., 1969).

[2]William E. Sharp, J. Geophys. Res. **76**, 987 (1971).

[3]A. L. Broadfoot and D. M. Hunten, Can. J. Phys. **42**, 1212 (1964).

[4]R. E. Miller, W. G. Fastie, and R. C. Isler, J. Geophys. Res. 73, 3353 (1968).

[5]P. N. Stanton and R. M. St. John, J. Opt. Soc. Am. 59, 252 (1969).

[6]D. J. Burns, F. R. Simpson, and J. W. McConkey, J. Phys. B 2, 52 (1969).

[7]D. E. Shemansky and A. L. Broadfoot, J. Quant. Spectr. Radiative Transfer 11, 1385 (1971); 11, 1401 (1971).

[8]D. C. Cartwright, Trans. Am. Geophys. Union 51, 791 (1970).

[9]D. C. Cartwright, Phys. Rev. A 2, 1331 (1970).

[10]D. C. Cartwright (private communication).

[11]Joseph M. Ajello, J. Chem. Phys. 53, 1156 (1970).

[12]R. S. Freund, J. Chem. Phys. 54, 1407 (1971).

[13]W. L. Borst, W. C. Wells, and E. C. Zipf (unpublished).

[14]W. L. Borst and E. C. Zipf, Phys. Rev. A 3, 979 (1971). For other experimental details, in particular the pressure calibration, see W. L. Borst and E. C. Zipf, Phys. Rev. A 1, 834 (1970). The cross section for the (0, 0) ING band of N_2^+ reported there served as a means of calibrating the absolute gas density in the present work

for which uniform pressure existed only in the reaction chamber but not in the entire vacuum chamber.

[15]W. L. Borst, Rev. Sci. Instr. 42, 1543 (1971).

[16]W. L. Borst and E. C. Zipf, Phys. Rev. A 4, 153 (1971).

[17]D. E. Shemansky, J. Chem. Phys. 51, 689 (1969).

[18]W. C. Wells, W. L. Borst, and E. C. Zipf, Chem. Phys. Letters (to be published).

[19]R. T. Brinkman and S. Trajmar, Ann. Geophys. (Rome) 26, 201 (1970).

[20]A. J. Williams III and John P. Doering, Planetary Space Sci. 17, 1527 (1969).

[21]R. S. Stolarski, V. A. L. Dulock, C. E. Watson, and A. E. S. Green, J. Geophys. Res. 72, 2353 (1967).

[22]E. Bauer and C. E. Bartky, J. Chem. Phys. 43, 2466 (1965).

[23]R. S. Freund, J. Chem. Phys. 51, 1979 (1969).

[24]F. A. Gilmore, Can. J. Chem. 47, 1779 (1969).

[25]D. E. Shemansky, E. C. Zipf, and T. M. Donahue, Planetary Space Sci. (to be published).

[26]John Olmsted III, Radiation Res. 31, 191 (1967).

[27]H. Ehrhardt and K. Willmann, Z. Physik 204, 462 (1967).

Production of Lyman-Alpha Radiation by 20- to 120-keV Hydrogen-Atom Impact on He, Ne, Ar, and N₂[†]

R. H. Hughes and Song-Sik Choe

Department of Physics, University of Arkansas, Fayetteville, Arkansas 72701

(Received 7 September 1971)

Absolute cross sections have been determined for the production of Lyman-α radiation by 20–120-keV ground-state hydrogen atoms impacting on He, Ne, Ar, and N₂. Atom impact on He follows the predicted energy dependence of Levy's Born wave calculation of $2p$ excitation beyond 30 keV. Although the experimental value remains about 25% higher than the theoretical value in this region, the agreement is well within experimental error. For Ne, Levy's scaled Born calculation for $2p$ excitation agrees reasonably well with experiment. However, it is particularly apparent for impact on Ar that the scaled Born calculation underestimates the excitation at the higher energies. All cross sections decrease more rapidly with energy initially than at the higher energies, where a characteristic flattening of the cross-section–vs–energy curve occurs, suggesting the importance of simultaneous excitation of the target and projectile atoms at these energies.

I. INTRODUCTION

Production of Lyman-α radiation by hydrogen atom impact on N₂ has been measured by Dahlberg et al.[1] for 20–130-keV impact, and by Birely and McNeal[2] below 30 keV. Similar measurements have been carried out on He, Ne, and Ar by Birely and McNeal[3] to 25 keV, by Dose et al.[4] to 55 keV, and by Orbeli et al.[5] to 40 keV. We extend the energy range in this investigation of these rare gases.

Levy has calculated the excitation of these rare gases using the Born wave method by describing the target atoms by elastic and inelastic x-ray form factors.[6] In the case of helium[6,7] he found excellent agreement with the experimental work of Orbeli

et al.[5] when the experimental values for $2s$ and $2p$ cross sections were summed over the entire experimental range of 5–40 keV. Some discrepancies became apparent when the two cross sections were treated separately. Levy also found that he could reasonably reproduce the $n = 2$ measurement of Ref. 5 for Ne, Ar, and Kr by scaling his Born calculation by a velocity-dependent factor obtained by a comparison of the theoretical ionization cross sections with the experimental values.[6,8]

Birely and McNeal[3] made $n = 2$ measurements for impact on the rare gases and discovered an apparent discrepancy in the helium work of Ref. 5. Both experiments used the same optical calibration, which is based on the charge-transfer work of